JOURNAL OF GUIDANCE, CONTROL, AND DYNAMICS
Vol. 37, No. 4, July–August 2014

Engineering Notes

Saturated Tracking Control of Store-Induced Limit Cycle Oscillations

B. J. Bialy* and L. Andrews†
University of Florida, Gainesville, Florida 32611
J. Willard Curtis‡
U.S. Air Force Research Laboratory, Eglin Air Force Base, Florida 32542
and
W. E. Dixon§
University of Florida, Gainesville, Florida 32611

DOI: 10.2514/1.G000325

I. Introduction

HIGH-PERFORMANCE fighter aircraft experience store-induced limit cycle oscillations (LCOs) [1], which are characterized by a limited amplitude, antisymmetric motion of the wing and lateral motion of the fuselage and cockpit. The main concern with LCO motion is its negative impact on a pilot's ability to complete a mission; specifically, the lateral motion of the cockpit causes difficulties when reading cockpit gauges and the head-up display [1]. Additional concerns arise over the ability to release ordnance during LCO motion and the effects of LCO on target acquisition for smart weapons and accuracy for unguided munitions [2]. The adverse effects of LCO behavior on flight performance necessitate the development of a control strategy capable of suppressing LCO motion.

Several control strategies have been developed to mitigate LCO behavior in an aeroelastic system requiring exact knowledge of the dynamics, including linear-quadratic regulator (LQR) [3–5], feedback linearization [6], linear multivariable control on a linear reduced-order model [7,8], and state-dependent Riccati equation and sliding-mode control approaches [9]. These controllers do not compensate for uncertainties in the aerodynamic and structural models or external disturbances and are restricted to specific flight regimes.

Adaptive controllers have been developed to compensate for structured uncertainties, including partial feedback linearization [10], model reference adaptive control (MRAC) [11], and structured MRAC [12]. Previous controllers considered structured uncertainties in the torsional stiffness model only. A robust integral of the sign of the error (RISE) controller was developed in the preliminary work in [13] to suppress LCO behavior in a two-degree-of-freedom (2DOF) airfoil section with uncertainties in the dynamics that can not be classified as linear-in-the-parameters and an additive, unknown nonlinear disturbance. A feedforward neural network is used to compensate for the system uncertainties, whereas a RISE feedback term guarantees asymptotic tracking of a desired angle of attack (AOA). Simulation results indicated that the maximum control effort is sensitive to variations in the system uncertainties, which could lead to unexpected actuator saturation during the transient period. Although the developed controller does compensate for modeling uncertainties and exogenous disturbances, it does not account for actuator limits.

Previously developed controllers that target the LCO problem have neglected the fact that the commanded input may exceed the actuation limits of the system. The objective in this Note is to develop a controller (based on the preliminary work by the authors in [14]) capable of mitigating LCO behavior in a 2DOF airfoil section in the presence of time-varying nonlinear disturbances and modeling uncertainties, while also compensating for actuator constraints. The current work builds on the control structure in [13]; however, the error system, control development, and stability analysis are all redesigned to compensate for the actuator constraints. Motivated by the desire to achieve an asymptotic tracking result in the presence of exogenous disturbances, the control development is based on a RISE-based control structure [15]. Furthermore, based on the desire to account for actuator saturation, the developed controller leverages the saturated RISE-based structure in [16]. Specifically, the theoretical architecture in [16] of embedding a RISE controller in a saturated hyperbolic function is adopted in this result, where the argument of the trigonometric function, and hence the resulting closed-loop error system, is modified to address the specific challenges of the LCO mitigation problem.

II. Aeroelastic Model

Consider an aeroelastic model of a 2DOF airfoil (see Fig. 1) given by [13,17]

$$M\ddot{q} + C\dot{q} + Kq = F \tag{1}$$

where $q \triangleq [\,h \quad \alpha\,]^T \in \mathbb{R}^2$ is a vector of the system states, where α and $h \in \mathbb{R}$ denote the vertical position of the airfoil section and the AOA of the airfoil section, respectively.

Based on the description of LCO behavior [2], the system states are bounded as $\|q\| \le \kappa_1$, $\|\dot{q}\| \le \kappa_2$, and $\|\ddot{q}\| \le \kappa_3$, where $\kappa_1, \kappa_2, \kappa_3 \in \mathbb{R}$ are known positive constants. In Eq. (1), the matrices $M \in \mathbb{R}^{2\times2}$, $C \in \mathbb{R}^{2\times2}$, $K \in \mathbb{R}^{2\times2}$, and the vector $F \in \mathbb{R}^2$ are defined as

$$M \triangleq \begin{bmatrix} m_1 & m_2 \\ m_2 & m_4 \end{bmatrix}, \qquad C \triangleq \begin{bmatrix} c_{h_1} & c_{h_2}\dot{\alpha} \\ 0 & c_\alpha \end{bmatrix} \tag{2}$$

$$K \triangleq \begin{bmatrix} k_h & 0 \\ 0 & k_\alpha \end{bmatrix}, \qquad F \triangleq \begin{bmatrix} -L \\ P_M \end{bmatrix} \tag{3}$$

The unknown constants m_1 and $m_4 \in \mathbb{R}$ from Eq. (2) are defined as

$$m_1 \triangleq m_s + m_w \tag{4}$$

$$m_4 \triangleq [(r_x - a)^2 + (r_h - a_h)^2]b^2 m_w + [(s_x - a)^2 + (s_h - a_h)^2]b^2 m_s + I_w + I_s \tag{5}$$

Presented as Paper 2013-4529 at the AIAA Guidance, Navigation, and Control Conference, Boston, MA, 19–22 August 2013; received 11 October 2013; revision received 8 January 2014; accepted for publication 19 January 2014; published online 30 April 2014.

*Graduate Research Assistant, Department of Mechanical and Aerospace Engineering; bialybj@ufl.edu.
†Graduate Research Assistant, Department of Mechanical and Aerospace Engineering; landr010@ufl.edu.
‡Technical Adviser, Munitions Directorate; jess.curtis@eglin.af.mil. Member AIAA.
§Professor, Department of Mechanical and Aerospace Engineering; wdixon@ufl.edu.

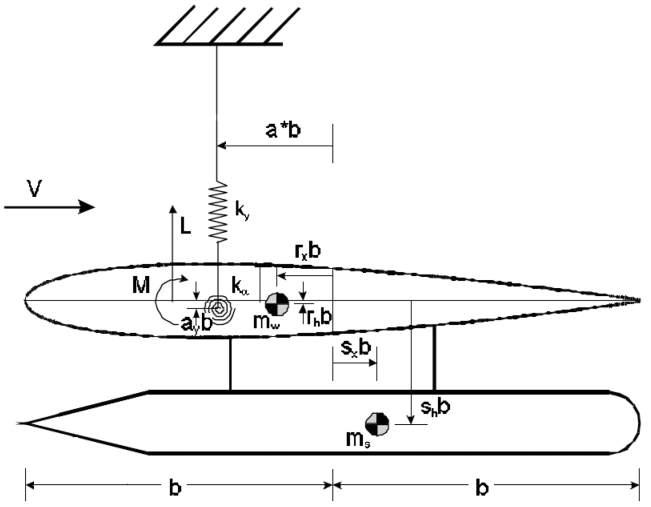

Fig. 1 Diagram of the 2DOF airfoil section based on that in [17].

and $m_2 \in \mathbb{R}$ is defined as

$$m_2 \triangleq (r_x - a)m_w b\,\cos(\alpha) + (s_x - a)m_s b\,\cos(\alpha) - (s_h - a_h)m_s b\,\sin(\alpha) - (r_h - a_h)m_w b\,\sin(\alpha) \tag{6}$$

where m_w, m_s, b, r_x, r_h, a, a_h, s_x, s_h, I_w, and $I_s \in \mathbb{R}$ are unknown constants. Specifically, m_w and m_s denote the mass of the airfoil section and store, respectively; b denotes the semichord of the airfoil, r_x and r_h represent the distance from the wing center of mass to the airfoil midchord and the distance from the store center of mass to the airfoil midchord in percentage of the wing semichord, respectively; a and a_h are the distances from the elastic axis of the airfoil section to the airfoil midchord and chord line in percentage of the wing semichord, respectively; s_x and s_h are the distances from the store center of mass to the wing midchord and chord line in percentage of the wing semichord, respectively; and I_w and I_s represent the wing and store moments of inertia, respectively. In Eq. (2), $c_\alpha \in \mathbb{R}$ and $c_{h_1} \in \mathbb{R}$ are the unknown damping coefficients in the AOA and vertical position motions, respectively, and $c_{h_2} \in \mathbb{R}$ is defined as [13]

$$c_{h_2} \triangleq -(r_x - a)m_w b\,\cos(\alpha) - (s_x - a)m_s b\,\cos(\alpha) - (s_h - a_h)m_s b\,\sin(\alpha) - (r_h - a_h)m_w b\,\sin(\alpha)$$

In Eq. (3), $k_h \in \mathbb{R}$ denotes the constant unknown stiffness coefficient in the vertical position, and $k_\alpha \in \mathbb{R}$ denotes the unknown nonlinear pitch stiffness coefficient and is modeled as

$$k_\alpha = k_{\alpha_1} + k_{\alpha_2}\alpha + k_{\alpha_3}\alpha^2 + k_{\alpha_4}\alpha^3 + k_{\alpha_5}\alpha^4 + k_{\alpha_6}\alpha^5$$

where the stiffness parameters $k_{\alpha_i} \in \mathbb{R}$, $i = 1, \ldots, 6$ are uncertain constants. In Eq. (3), $L \in \mathbb{R}$ and $P_M \in \mathbb{R}$ are modeled as

$$L = \rho U^2 b S C_{l_\alpha}\alpha_{\text{ef}} + C_{l_\delta}\delta \tag{7}$$

$$P_M = \rho U^2 b^2 S C_{l_\alpha}\left(\frac{1}{2} + a\right)\alpha_{\text{ef}} + C_{m_\delta}\delta \tag{8}$$

where $\rho \in \mathbb{R}$ denotes the constant unknown atmospheric density; $U \in \mathbb{R}$ denotes the constant unknown freestream velocity; $S \in \mathbb{R}$ represents a constant unknown reference length; C_{l_α}, C_{l_δ}, and $C_{m_\delta} \in \mathbb{R}$ denote the constant unknown airfoil lift coefficient, control surface lift coefficient, and control surface pitch moment coefficient, respectively; $\delta \in \mathbb{R}$ represents the control surface deflection angle; and $\alpha_{\text{ef}} \in \mathbb{R}$ represents the effective AOA and is modeled as

$$\alpha_{\text{ef}} \triangleq \alpha + \frac{\dot{h}}{U} + \frac{b(\frac{1}{2} - a)\dot{\alpha}}{U}$$

The system dynamics in Eq. (1) can be expressed as [see [13] for details on the existence of $M^{-1}(\alpha)$]

$$\ddot{q} = M^{-1}(C_\delta\delta - \tilde{C}\,\dot{q} - \tilde{K}q) + d \tag{9}$$

where $C_\delta \triangleq [-C_{l_\delta} \quad C_{m_\delta}]^T \in \mathbb{R}^2$, $d \triangleq [d_h \quad d_\alpha]^T \in \mathbb{R}^2$ denotes an unknown nonlinear disturbance that represents unmodeled, unsteady aerodynamic effects, and $\tilde{C}$, $\tilde{K} \in \mathbb{R}^{2\times 2}$ are defined as

$$\tilde{C} \triangleq \begin{bmatrix} c_{h_1} + C_L & c_{h_2}\dot{\alpha} + C_L b\left(\frac{1}{2} - a\right) \\ -C_L b\left(\frac{1}{2} + a\right) & c_\alpha - C_L b^2\left(\frac{1}{4} - a^2\right) \end{bmatrix} = \begin{bmatrix} \tilde{C}_{11} & \tilde{C}_{12} \\ \tilde{C}_{21} & \tilde{C}_{22} \end{bmatrix},$$

$$\tilde{K} \triangleq \begin{bmatrix} k_h & C_L U \\ 0 & k_\alpha - C_L U b\left(\frac{1}{2} + a\right) \end{bmatrix} = \begin{bmatrix} \tilde{K}_{11} & \tilde{K}_{12} \\ 0 & \tilde{K}_{22} \end{bmatrix}$$

and $C_L \triangleq \rho U b S C_{l_\alpha} \in \mathbb{R}$ is an unknown constant. The subsequent control development is based on the assumption that the nonlinear disturbances are bounded as

$$|d_h| \le \xi_1, \qquad |\dot{d}_h| \le \xi_2, \quad |d_\alpha| \le \xi_3, \qquad |\dot{d}_\alpha| \le \xi_4$$

where $\xi_j \in \mathbb{R}$, $(j = 1, \ldots, 4)$ are positive, known constants.

III. Control Objective

The objective is to develop a limited amplitude continuous controller that guarantees asymptotic tracking of the airfoil section AOA. The subsequent development is based on the assumption that $\alpha_d, \dot{\alpha}_d, \ddot{\alpha}_d, \alpha_d, \alpha_d \in L_\infty$, where $\alpha_d \in \mathbb{R}$ denotes the desired AOA trajectory. The control objective is quantified by defining a tracking error $e_1 \in \mathbb{R}$ as

$$e_1 \triangleq \alpha - \alpha_d \tag{10}$$

To facilitate the control design, the auxiliary tracking errors e_2, $r \in \mathbb{R}$ are defined as [16]

$$e_2 \triangleq \dot{e}_1 + \gamma_1\,\tanh(e_1) + \tanh(e_f) \tag{11}$$

$$r \triangleq \dot{e}_2 + \gamma_2\,\tanh(e_2) + \gamma_3 e_2 \tag{12}$$

where $\gamma_1, \gamma_2, \gamma_3 \in \mathbb{R}$ are positive constant control gains, and the auxiliary signal $e_f \in \mathbb{R}$ is defined as the solution to the following differential equation [16]:

$$\dot{e}_f \triangleq \cosh^2(e_f)[-\gamma_4 e_2 + \tanh(e_1) - \gamma_5\,\tanh(e_f)], \quad e_f(t_0) = e_{f_o} \tag{13}$$

where $e_{f_o} \in \mathbb{R}$ is a known initial condition, and $\gamma_4, \gamma_5 \in \mathbb{R}$ are positive constant control gains. The subsequent development is based on the assumption that q and $\dot{q}$ are measurable; hence, e_1 and e_2 are measurable, and e_f can be computed from measurable terms, but r is not measurable or known because it depends on $\ddot{q}$. The following inequality properties [18] will be used in the subsequent development:

$$|\xi| \ge |\tanh(\xi)|, \qquad |\tanh(\xi)|2 \ge \tanh^2(|\xi|) \tag{14}$$

$$\xi\,\tanh(\xi) \ge \tanh^2(\xi), \qquad |\xi|2 \ge \ln[\cosh(\xi)] \ge \frac{1}{2}\tanh^2(|\xi|) \tag{15}$$

IV. Control Development

Substituting the dynamics from Eq. (9) into Eq. (12) and multiplying by $\det(M)/g$ yields

$$\frac{\det(M)}{g}r = \frac{f}{g} + \frac{\det(M)}{g}d_\alpha + \delta \tag{16}$$

where the auxiliary terms $f \in \mathbb{R}$ and $g \in \mathbb{R}$ are defined as

$$\begin{aligned} f \triangleq & -m_1(\tilde{C}_{21}\dot{h} + \tilde{C}_{22}\dot{\alpha} + \tilde{K}_{22}\alpha) + m_2(\tilde{C}_{11}\dot{h} + \tilde{C}_{12}\dot{\alpha} \\ & + \tilde{K}_{11}h + \tilde{K}_{12}\alpha) - \det(M)\ddot{\alpha}_d + \det(M)\gamma_1\cosh^{-2}(e_1) \\ & \times [e_2 - \gamma_1\tanh(e_1) - \tanh(e_f)] - \det(M)\gamma_5\tanh(e_f) \\ & + \det(M)[\tanh(e_1) + \gamma_2\tanh(e_2) + \gamma_3 e_2 - \gamma_4 e_2], \\ g \triangleq & \, m_2 C_{l_\delta} + m_1 C_{m_\delta} \end{aligned}$$

The auxiliary term g is positive, provided the sufficient conditions on the airfoil geometry and store location in [13] are satisfied.

Based on the open-loop error system in Eq. (16), the control surface deflection is designed as [16]

$$\delta = -\gamma_4\tanh(v) \tag{17}$$

where $v \in \mathbb{R}$ is the generalized Filippov solution to the following differential equation:

$$\dot{v} = \beta\cosh^2(v)\mathrm{sgn}(e_2), \qquad v(t_0) = v_o \tag{18}$$

where $\beta \in \mathbb{R}$ is a constant positive control gain and $v_o \in \mathbb{R}$ is a known initial condition. The theory of differential inclusions in [19] and ([20] Chapter 4) can be used to show the existence of solutions for $\dot{v} \in K[w_1]$, where $w_1\colon \mathbb{R} \to \mathbb{R}$ is defined as the right-hand side of Eq. (18),

$$K[w_1] \triangleq \bigcap_{\tau>0}\bigcap_{\mu S_m=0}\overline{co}\, w_1(e_1, B - S_m)$$

and

$$\bigcap_{\mu S_m=0}$$

denotes the intersection of sets of Lebesque measure zero, $\overline{co}$ represents convex closure, and $B = \{\varepsilon \in \mathbb{R} || e_2 - \varepsilon| < \tau\}$ [21,22]. From Eq. (17), it is clear that the control input is bounded and will not breach the actuator limitations provided the control gain γ_4 is selected to be less than the actuator limit. Motivation for the use of the hyperbolic tangent function in Eq. (17) stems from the desire to inject a smooth saturation function into the control structure. The design of the auxiliary term v in Eq. (18) is motivated by the extra derivative that will be applied to the closed-loop system in Eq. (16), which is typical in RISE analysis methods. The extra derivative will introduce a $\cosh^{-2}(v)$ term in the closed-loop dynamics that will be canceled by the $\cosh^2(v)$ in Eq. (18).

The closed-loop tracking error can be obtained by taking the time derivative of Eq. (16) and substituting the time derivative of Eq. (17) to yield

$$\begin{aligned} \frac{\det(M)}{g}\dot{r} = & -\frac{1}{2}\frac{\mathrm{d}}{\mathrm{d}t}\left(\frac{\det(M)}{g}\right)r + \tilde{N} + N_d + \Omega - \tanh(e_2) \\ & - e_2 - \frac{\det(M)}{g}\gamma_4 r - \beta\gamma_4\,\mathrm{sgn}(e_2) \end{aligned} \tag{19}$$

where $\tilde{N} \in \mathbb{R}$, $N_d \in \mathbb{R}$, and $\Omega \in \mathbb{R}$ are defined as

$$\begin{aligned} \tilde{N} \triangleq & -\frac{1}{2}\frac{\mathrm{d}}{\mathrm{d}t}\left(\frac{\det(M)}{g}\right)r + \frac{\mathrm{d}/\mathrm{d}t[\det(M)]}{g}\gamma_1\cosh^{-2}(e_1) \\ & \times [e_2 - \gamma_1\tanh(e_1) - \tanh(e_f)] \\ & - \frac{2\det(M)}{g}\gamma_1\cosh^{-2}(e_1)\tanh(e_1)\dot{e}_1^2 \\ & - \frac{\det(M)}{g}\gamma_1 2\cosh^{-4}(e_1)\dot{e}_1 + \tanh(e_2) + e_2 \\ & - \frac{\det(M)}{g2}C_{l_\delta}\dot{m}_2[\gamma_1\cosh^{-2}(e_1)\dot{e}_1 - \gamma_5\tanh(e_f) + \tanh(e_1) \\ & + \gamma_2\tanh(e_2) + \gamma_3 e_2] \\ & - \frac{\mathrm{d}/\mathrm{d}t[\det(M)]}{g}[\gamma_5\tanh(e_f) - \tanh(e_1) - \gamma_2\tanh(e_2) - \gamma_3 e_2] \\ & - \frac{\det(M)}{g}[\gamma_5\tanh(e_1) - \gamma_5^2\tanh(e_f) - \cosh^{-2}(e_1)\dot{e}_1 \\ & - \gamma_2\cosh^{-2}(e_2)\dot{e}_2 - \gamma_3\dot{e}_2] \\ & + \frac{\det(M)}{g}\gamma_1\cosh^{-2}(e_1)[\dot{e}_2 - \tanh(e_1) + \gamma_5\tanh(e_f)] \end{aligned} \tag{20}$$

$$\begin{aligned} N_d \triangleq & \frac{\dot{m}_2}{g}(\tilde{C}_{11}\dot{h} + \tilde{C}_{12}\dot{\alpha} + \tilde{K}_{11}h + \tilde{K}_{12}\alpha) - \frac{m_1}{g}(\tilde{C}_{21}\ddot{h} + \tilde{C}_{22}\ddot{\alpha} \\ & + \tilde{K}_{22}\dot{\alpha} + \dot{\tilde{K}}_{22}\alpha) - \frac{\det(M)}{g}\alpha_d + \frac{m_2}{g}(\tilde{C}_{11}\ddot{h} + \tilde{C}_{12}\ddot{\alpha} \\ & + \dot{\tilde{C}}_{12}\dot{\alpha} + \tilde{K}_{11}\dot{h} + \tilde{K}_{12}\dot{\alpha}) - \frac{\mathrm{d}/\mathrm{d}t[\det(M)]}{g}\ddot{\alpha}_d + \frac{\mathrm{d}}{\mathrm{d}t}\left(\frac{\det(M)}{g}\right)d_\alpha \\ & + \frac{\det(M)}{g}\dot{d}_\alpha + \frac{C_{l_\delta}\dot{m}_2}{g2}[m_1(\tilde{C}_{21}\dot{h} + \tilde{C}_{22}\dot{\alpha} + \tilde{K}_{22}\alpha) \\ & - m_2(\tilde{C}_{11}\dot{h} + \tilde{C}_{12}\dot{\alpha} + \tilde{K}_{11}h + \tilde{K}_{12}\alpha) + \det(M)\ddot{\alpha}_d) \end{aligned} \tag{21}$$

$$\begin{aligned} \Omega \triangleq & \gamma_4 e_2\left[\frac{\det(M)}{g}(\gamma_1\cosh^{-2}(e_1) + \gamma_5 + \gamma_3) - \frac{\mathrm{d}/\mathrm{d}t[\det(M)]}{g}\right. \\ & \left. + \frac{\dot{m}_2 C_{l_\delta}\det(M)}{g2}\right] + \frac{\det(M)}{g}\gamma_2\gamma_4\tanh(e_2) \end{aligned} \tag{22}$$

Using the assumptions on the desired trajectories and boundedness of the LCO states, upper bounds can be developed for Eqs. (20) and (21) as

$$|\tilde{N}| \le \zeta_0\|x\|, \qquad |N_d| \le \zeta_1, \qquad |\dot{N}_d| \le \zeta_2 \tag{23}$$

where $\zeta_0, \zeta_1, \zeta_2 \in \mathbb{R}$ are known bounding constants, and $x \in \mathbb{R}4$ is defined as

$$x \triangleq [\,\tanh(e_1) \quad e_2 \quad r \quad \tanh(e_f)\,]^T \tag{24}$$

V. Stability Analysis

Theorem 1: The controller given in Eqs. (17) and (18) yields asymptotic tracking in the sense that all Filippov solutions to the differential equations in Eqs. (11–13) and (19) are bounded and satisfy $e_1 \to 0$ as $t \to \infty$, provided that the control gains are selected as

$$\begin{aligned} & \gamma_1 > \frac{1}{2}, \qquad \gamma_3 > \gamma_4^2 + 1, \qquad \beta\gamma_4 > \zeta_1 + \frac{\zeta_2}{\gamma_3}, \\ & \lambda_1\gamma_a > \frac{c_1^2}{2}, \qquad \gamma_5 > \frac{\gamma_4^2}{2}, \qquad \lambda > \frac{\zeta_0^2}{4\lambda_1\gamma_b} \end{aligned} \tag{25}$$

where

$$\lambda \triangleq \min\left\{\gamma_1 - \frac{1}{2}, 2\gamma_2 + \gamma_3, \gamma_3 - \gamma_4^2 - 1, \lambda_1\gamma_a - \frac{c_1^2}{2}, \gamma_5 - \frac{\gamma_4^2}{2}\right\}$$

where c_1 and $\lambda_1 \in \mathbb{R}$ are positive bounding constants, where $\lambda_1 \leq [\det(M)/g]$ and

$$c_1 \geq \left|\left[\frac{\det(M)}{g}(\gamma_1 + \gamma_3 + \gamma_5) - \frac{\mathrm{d}/\mathrm{d}t[\det(M)]}{g} + \frac{\dot{m}_2 C_{l_\delta}\det(M)}{g^2}\right]^2 + \left(\gamma_2\frac{\det(M)}{g}\right)^2\right|,$$
$$\geq [c_{m_1}(\gamma_1 + \gamma_3 + \gamma_5) + c_{m_2} + c_{m_3}C_{l_\delta}]^2 + \gamma_2^2 c_{m_1}^2$$

where

$$c_{m_1} > \frac{\det(M)}{g}, \quad c_{m_2} > \frac{\mathrm{d}/\mathrm{d}t(\det(M))}{g}, \quad \text{and} \quad c_{m_3} > \frac{\dot{m}_2\det(M)}{g2}$$

(See Appendix for details.)

Remark 1: The control gains γ_1 and γ_2 can be selected independently of the remaining control gains and γ_4 is selected less than the actuator limit. After γ_4 is selected, the lower bounds on γ_3, γ_5, and β can be calculated. The selection of γ_a depends on the severity of the LCO motion which is captured in the constant c_1. If the LCO motion is too severe, the gain condition for γ_a cannot be satisfied without increasing the saturation limit.

Proof: See [16] for details.

VI. Numerical Simulations

A numerical simulation is presented to illustrate the performance of the developed controller and to provide a comparison with the controller in [13]. The controller in [13] is given by

$$\delta = -\frac{\hat{f}_d}{g_d} - \mu \tag{26}$$

where $\hat{f}_d/g_d \triangleq \hat{W}^T\sigma(\hat{V}^T x_d) \in \mathbb{R}$ is a neural network (NN) feedforward term used to approximate the unknown structural and aerodynamic parameters, $\hat{W} \in \mathbb{R}^{n_2+1}$ and $\hat{V} \in \mathbb{R}^{6\times n_2}$ are estimates of the ideal NN weights, σ: $\mathbb{R}^6 \to \mathbb{R}^{n_2+1}$ denotes a NN activation function, $n_2 \in \mathbb{R}$ denotes the number of neurons in the hidden layer of the NN, and $x_d \in \mathbb{R}^6$ represents the inputs to the NN. The ideal NN weight estimates are updated according to the update laws defined as

$$\dot{\hat{W}} \triangleq \mathrm{proj}(\Gamma_1\hat{\sigma}'\hat{V}^T\dot{x}_d e_2) \tag{27}$$

$$\dot{\hat{V}} \triangleq \mathrm{proj}[\Gamma_2\dot{x}_d(\hat{\sigma}'^T\hat{W}e_2)^T] \tag{28}$$

where $\Gamma_1 \in \mathbb{R}^{(n_2+1)\times(n_2+1)}$ and $\Gamma_2 \in \mathbb{R}^{6\times 6}$ are constant positive-definite control gain matrices, and

$$\hat{\sigma}' \triangleq \frac{\mathrm{d}\sigma(\hat{V}^T x_d)}{\mathrm{d}(\hat{V}^T x_d)}$$

Moreover, in Eq. (26), $\mu \in \mathbb{R}$ denotes the RISE feedback term defined as

$$\mu \triangleq k_s e_2 - k_s e_2(0) + v, \quad \dot{v} \triangleq k_s\alpha_2 e_2 + \beta_1\,\mathrm{sgn}(e_2), \qquad v(t_0) = v_0$$

where k_s, α_2, and $\beta_1 \in \mathbb{R}$ are constant positive control gains, and $v_0 \in \mathbb{R}$ is a known initial condition.

The model parameters for the simulation are shown in Table 1. The open-loop system was simulated with the following initial conditions: $h(0) = 0$ m, $\dot{h}(0) = 0$ m/s, $\alpha(0) = 11.5$ deg, and $\dot{\alpha}(0) = 0$ deg/s. It is evident from Fig. 2 that the open-loop system, under the preceding initial conditions and no exogenous disturbances, experiences LCO behavior.

Table 1 Aeroelastic model parameters

Parameter	Value	Parameter	Value
m_w	4.0 kg	k_h	2200 N/m
m_s	4.0 kg	k_{α_1}	0.5 N/rad
r_x	0.0	k_{α_2}	−11.05 N/rad^2
r_h	0.0	k_{α_3}	657.75 N/rad^3
a	−0.6	k_{α_4}	−4290 N/rad^4
a_h	0.0	k_{α_5}	8644.85 N/rad^5
b	0.14 m	k_{α_6}	0.0 N/rad^6
s_x	0.098	ρ	1.225 kg/m^3
s_h	1.4	U	15 m/s
I_w	0.043 kg · m^2	S	1.0 m
I_s	0.0050 kg · m^2	C_{l_α}	6.8 1/rad
c_{h_1}	27.43 kg/s	C_{l_δ}	93 N/rad
c_α	0.036 kg · m^2/s	C_{m_δ}	2.3 N · m/rad

The control objective in the subsequent numerical simulations is to regulate the AOA to 0 deg. In addition, an external disturbance, selected as $d(t) = [0 \quad 0.25\sin(t)]^T$, was added to the numerical simulation and a zero-mean noise signal uniformly distributed over an interval was added to each measurement. For the vertical displacement and velocity, the interval was $\pm 2.5 \times 10^{-3}$ m and $\pm 2.5 \times 10^{-3}$ m/s, respectively. For the AOA and AOA rate, the interval was $\pm 4.5 \times 10^{-2}$ rad and $\pm 1 \times 10^{-2}$ rad/s. Based on the identification performance of the NN, the NN feedforward parameters for the controller developed in [13] were selected as $n_2 = 25$, $\Gamma_1 = 10I_{26}$, and $\Gamma_2 = 10I_7$, where I_m denotes an $m \times m$ identity matrix. The RISE feedback control gains for the controller developed in [13] were determined through a 1500 sample Monte Carlo simulation in which the RISE feedback control gains for each sample were selected at random from within a specified interval. The gains used in the comparison study were selected as those that returned the minimum value for the following cost function

$$J = \sqrt{\frac{1}{n}\left[\sum_{i=1}^{n}\alpha 2(t_i)\right]} \tag{29}$$

where n is the total number of time steps in the numerical simulation. The set of control gains that produced the smallest AOA rms error were $\alpha_2 = 3.9513$, $k_s = 2.6112$, and $\beta_1 = 0.9966$. Figures 3 and 4 depict the performance of the unsaturated RISE controller developed in [13] and that same RISE controller with an ad hoc saturation applied to the commanded control. Although the unsaturated controller

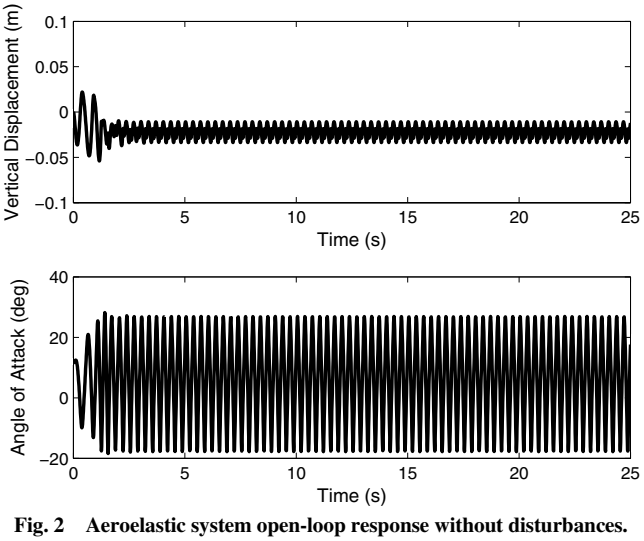

Fig. 2 Aeroelastic system open-loop response without disturbances.

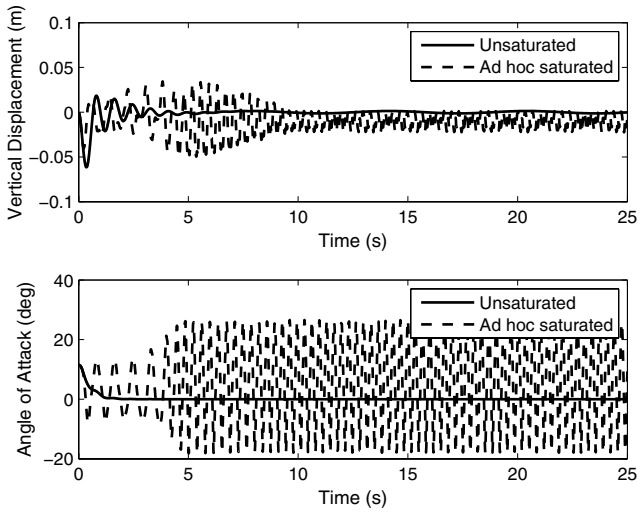

Fig. 3 State trajectories of the controller developed in [13] with and without saturation.

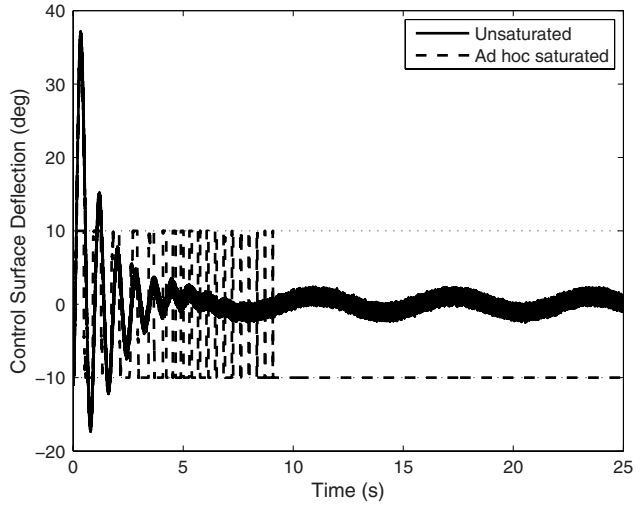

Fig. 4 Commanded control effort for the controller developed in [13] with and without saturation.

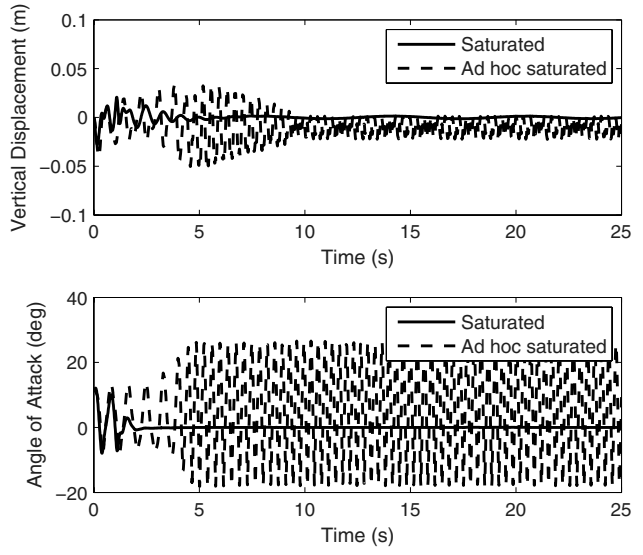

Fig. 5 State trajectories of the controller in [13] and the developed saturated controller.

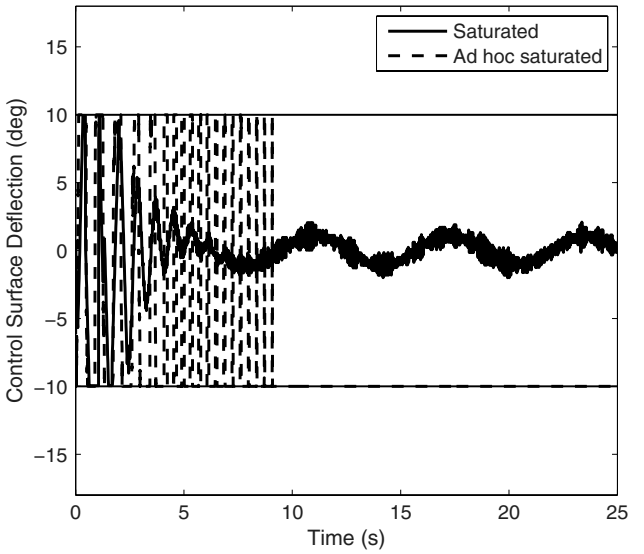

Fig. 6 Commanded control effort of the controller in [13] and the developed saturated controller.

suppressed the LCO behavior, the commanded control effort breached the actuator limit several times. When the ad hoc saturation was applied to the controller, the LCO behavior could not be suppressed and the system returned to an LCO state. In fact, after approximately 9 s, the ad hoc controller saturates at the lower limit for the remainder of the simulation. This highlights the unpredictable response that can occur when applying an ad hoc saturation without considering the stability of the resulting closed-loop system.

The developed control strategy was applied to the system with the following gains: $\gamma_1 = 0.8375$, $\gamma_2 = 17.7604$, $\gamma_3 = 33.9025$, $\gamma_4 = 0.1745$, $\gamma_5 = 15.4652$, and $\beta = 5.5539$. Note that γ_4 represents the actuator limit in radians, which was taken to be ± 10 deg. The control gains for the developed controller were determined by applying the same Monte Carlo approach used to select the gains for the controller in [13].

The states and control surface deflection of the ad hoc saturated controller and the developed saturated controller are shown in Figs. 5 and 6, respectively. Although different gain selections will alter the performance, Figs. 5 and 6 illustrate that the developed control strategy is capable of suppressing LCO behavior in the presence of actuator limits. The benefit of the developed method is that the saturation limit is included in the stability analysis, guaranteeing asymptotic tracking, versus the ad hoc saturation which yields an unpredictable response.

A 1500 sample Monte Carlo simulation was also performed to demonstrate the robustness of the developed saturated controller to plant uncertainties and measurement noise (see Table 2). The model parameters were varied uniformly over a range that extended from 95 to 105% of the parameter values listed in Table 1. Although the developed saturated controller successfully regulated the AOA for all 1500 samples, the transient performance varied significantly between samples.

The system states and control surface deflection for all 1500 samples are shown in Figs. 7–9. Figure 7 indicates that the AOA for most samples converges to zero after approximately 7 s, however, the considered range of model uncertainties does impact the transient performance of the controller. The sensitivity in transient performance can be attributed to the saturation on the commanded control

Table 2 Monte Carlo simulation results

	Mean, deg	Standard deviation, deg
Maximum tracking error	12.72	3.04
Rms tracking error	2.13	2.53

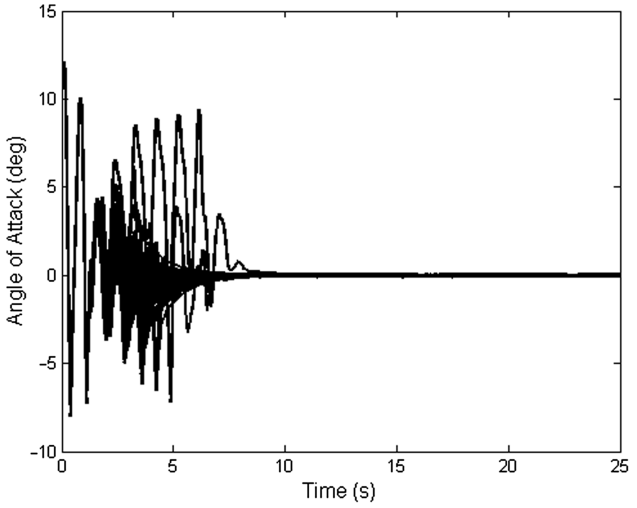

Fig. 7 AOA trajectories for all 1500 Monte Carlo samples.

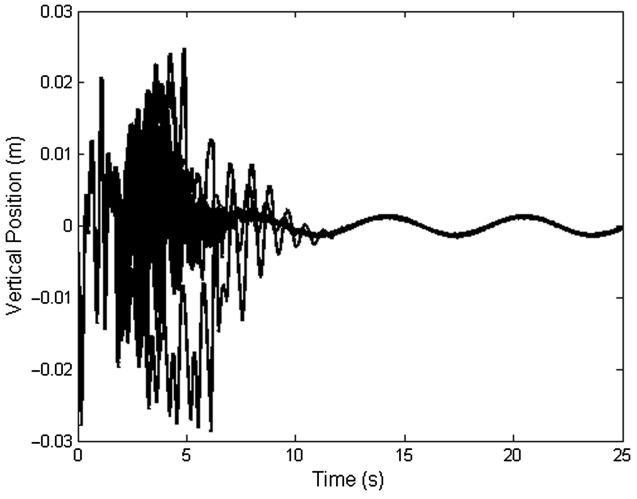

Fig. 8 Vertical position trajectories of all 1500 Monte Carlo samples.

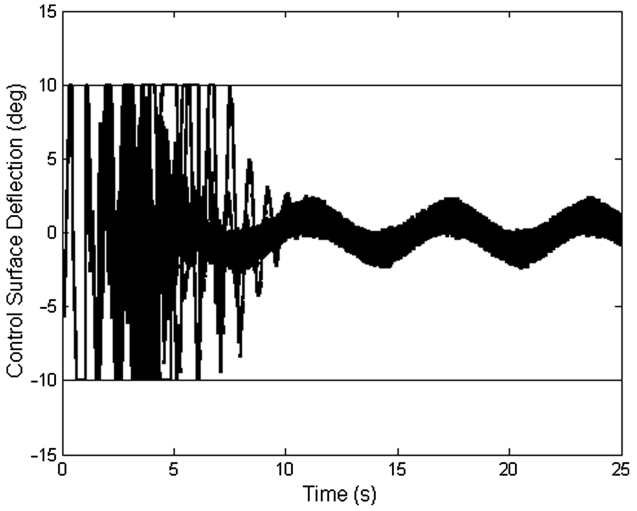

Fig. 9 Control surface deflection for all 1500 Monte Carlo samples.

effort. As noted previously, under certain conditions, the severity of the LCO can become more than the saturated controller can suppress and the system will return to an LCO state. From the figures, it is clear that some of the samples were close to producing LCOs that the saturated controller could not suppress.

VII. Conclusions

This Note presents a robust control strategy for the suppression of LCO behavior in an airfoil section. The control strategy uses a saturated RISE controller to asymptotically track a desired AOA trajectory without exceeding actuator limits. A Lyapunov-based stability analysis guarantees asymptotic tracking in the presence of actuator constraints, exogenous disturbances, and modeling uncertainties. Simulation results are presented to illustrate the performance of the developed control strategy. A numerical simulation was presented that demonstrated the unpredictable closed-loop system response when an ad hoc saturation strategy is applied to a previously developed controller. A comparison study revealed that the saturated controller developed in this Note achieved asymptotic tracking of the desired AOA trajectory, whereas the ad hoc saturation strategy was unable to suppress the LCO behavior. A 1500 sample Monte Carlo simulation was presented to demonstrate the robustness of the developed controller to variations in the model parameters. A potential drawback of the developed control strategy is that, under certain conditions, the severity of the produced LCO may result in sufficient gain conditions that cannot be satisfied. That is, if the disturbances to the system are large enough, then the system could be destabilized. This is a direct result of the actuator limit; increasing the actuator limit relaxes the sufficient gain conditions and allows for larger disturbances. Furthermore, an adaptive feedforward term could potentially be included to compensate for the uncertain dynamics, thereby relaxing the sufficient gain conditions. However, for any controller that has restricted control authority, it is possible for some disturbance to dominate the controller's ability to yield a desired or even stable performance.

There is a lack of clarity among researchers regarding the driving mechanism behind LCO. As in the work in [17], the LCO symptoms are captured by including a nonlinear torsional stiffness. As the driving mechanism of LCO is better understood, higher fidelity models can be used with the control structure developed in this work because the developed controller does not require knowledge of the model parameters, only upper bounds on the modeling uncertainties. The only change would be to modify the sufficient gain conditions to reflect the addition of the upper bounds on the uncertainties associated with the driving mechanism.

Future efforts are focused on improving the accuracy of the system model by considering the wing as a cantilevered beam undergoing bending and twisting deformations. This model will capture LCO behavior in a flexible wing, rather than a 2DOF airfoil section, using a set of partial differential equations. Boundary control techniques will then be used to suppress LCO motion in the flexible-wing model. As the driving mechanism behind LCO is better understood, that knowledge can be incorporated into the flexible-wing model and boundary control techniques to provide a more complete control strategy for suppressing LCO behavior.

Appendix: Details on the Development of the Constants c_{m_1}, c_{m_2}, and c_{m_3}

Using the results of ([13] Appendix B), $g > \varepsilon_1$ where $\varepsilon_1 \in \mathbb{R}$ is a known positive constant. The determinant of M can be expressed as $\det(M) = m_1 m_4 - m_2^2$. Since $m_2^2 \geq 0$, $|\det(M)| \leq m_1 m_4$ and

$$\left|\frac{\det(M)}{g}\right| \leq \frac{m_1 m_4}{\varepsilon_1} < c_{m_1}$$

Taking the time derivative of $\det(M)$ yields

$$\begin{aligned}\frac{\mathrm{d}}{\mathrm{d}t}[\det(M)] &= -2m_2\dot{m}_2 \\ &= 2m_2 m_w b\dot{\alpha}(r_h - a_h)\cos(\alpha) \\ &\quad + 2m_2 m_w b\dot{\alpha}(r_x - a)\sin(\alpha) \\ &\quad + 2m_2 m_s b\dot{\alpha}(s_h - a_h)\cos(\alpha) \\ &\quad + 2m_2 m_s b\dot{\alpha}(s_x - a)\sin(\alpha)\end{aligned}$$

Since $\|\dot{q}\| \leq \kappa_2$ and using the result in ([13] Appendix B), the time derivative of $\det(M)$ can be upper bounded as

$$\frac{\mathrm{d}}{\mathrm{d}t}[\det(M)] < \varepsilon_2$$

where $\varepsilon_2 \in \mathbb{R}$ is a known positive constant. Since $g > \varepsilon_1$,

$$\frac{\mathrm{d}/\mathrm{d}t[\det(M)]}{g}$$

can be upper bounded as

$$\left|\frac{\mathrm{d}/\mathrm{d}t[\det(M)]}{g}\right| \leq \frac{\varepsilon_2}{\varepsilon_1} = c_{m_2}$$

Using the result in ([13] Appendix B) and the upper bound on $\mathrm{d}/\mathrm{d}t[\det(M)]$, $\dot{m}_2$ can be upper bounded as $\dot{m}_2 \leq \varepsilon_3$, where $\varepsilon_3 \in \mathbb{R}$ is a known positive constant. Using ([13] Appendix B), the term

$$\frac{\dot{m}_2 C_{l_\delta} \det(M)}{g^2}$$

can be upper bounded as

$$\frac{\dot{m}_2 C_{l_\delta} \det(M)}{g^2} \leq \frac{\varepsilon_3 C_{l_\delta} \varepsilon_4}{\varepsilon_1^2} < c_{m_3}$$

where $\varepsilon_4 > |\det(M)|$.

Acknowledgments

This research is supported by a SMART fellowship and a contract with U.S. Air Force Research Laboratory Mathematical Modeling and Optimization Institute at Eglin Air Force Base. Any opinions, findings, and conclusions or recommendations expressed in this material are those of the authors and do not necessarily reflect the views of the sponsoring agency.

References

[1] Beran, P. S., Strganac, T. W., Kim, K., and Nichkawde, C., "Studies of Store-Induced Limit Cycle Oscillations Using a Model with Full System Nonlinearities," *Nonlinear Dynamics*, Vol. 37, No. 4, 2004, pp. 323–339. doi:10.1023/B:NODY.0000045544.96418.bf

[2] Bunton, R. W., and Denegri, C. M. Jr., "Limit Cycle Oscillation Characteristics of Fighter Aircraft," *Journal of Aircraft*, Vol. 37, No. 5, 2000, pp. 916–918. doi:10.2514/2.2690

[3] Block, J. J., and Strganac, T. W., "Applied Active Control for a Nonlinear Aeroelastic Structure," *Journal of Guidance, Control, and Dynamics*, Vol. 21, No. 6, 1999, pp. 838–845.

[4] Zhang, W., and Ye, Z., "Control Law Design for Transonic Aeroservoelasticity," *Aerospace Science and Technology*, Vol. 11, Nos. 2–3, 2007, pp. 136–145. doi:10.1016/j.ast.2006.12.004

[5] Prime, Z., Cazzolato, B., Doolan, C., and Strganac, T., "Linear-Parameter-Varying Control of an Improved Three-Degree-of-Freedom Aeroelastic Model," *Journal of Guidance, Control, and Dynamics*, Vol. 33, No. 2, 2010, pp. 615–618. doi:10.2514/1.45657

[6] Ko, J., Strganac, T. W., and Kurdila, A., "Stability and Control of a Structurally Nonlinear Aeroelastic System," *Journal of Guidance, Control, and Dynamics*, Vol. 21, No. 5, 1998, pp. 718–725. doi:10.2514/2.4317

[7] Danowsky, B. P., Thompson, P. M., Farhat, C., Lieu, T., Harris, C., and Lechniak, J., "Incorporation of Feedback Control into a High-Fidelity Aeroservoelastic Fighter Aircraft Model," *Journal of Aircraft*, Vol. 47, No. 4, 2010, pp. 1274–1282. doi:10.2514/1.47119

[8] Thompson, P. M., Danowsky, B. P., Farhat, C., Lieu, T., Lechniak, J., and Harris, C., "High-Fidelity Aeroservoelastic Predictive Analysis Capability Incorporating Rigid Body Dynamics," *Proceedings of the AIAA Atmospheric Flight Mechanics Conference*, AIAA Paper 2011-6209, 2011.

[9] Elhami, M. R., and Narab, M. F., "Comparison of SDRE and SMC Control Approaches for Flutter Suppression in a Nonlinear Wing Section," *Proceedings of the American Control Conference*, IEEE Publications, Piscataway, NJ, 2012, pp. 6148–6153.

[10] Ko, J., Strganac, T. W., and Kurdila, A., "Adaptive Feedback Linearization for the Control of a Typical Wing Section with Structural Nonlinearity," *Nonlinear Dynamics*, Vol. 18, No. 3, 1999, pp. 289–301.

[11] Platanitis, G., and Strganac, T. W., "Control of a Nonlinear Wing Section Using Leading- and Trailing-Edge Surfaces," *Journal of Guidance, Control, and Dynamics*, Vol. 27, No. 1, 2004, pp. 52–58. doi:10.2514/1.9284

[12] Strganac, T. W., Ko, J., Thompson, D. E., and Kurdila, A., "Identification and Control of Limit Cycle Oscillations in Aeroelastic Systems," *Journal of Guidance, Control, and Dynamics*, Vol. 23, No. 6, 2000, pp. 1127–1133. doi:10.2514/2.4664

[13] Bialy, B. J., Pasiliao, C. L., Dinh, H. T., and Dixon, W. E., "Lyapunov-Based Tracking of Store-Induced Limit Cycle Oscillations in an Aeroelastic System," *Proceedings of ASME Dynamic Systems and Control Conference*, American Society of Mechanical Engineers, New York, Oct. 2012, pp. 803–811.

[14] Bialy, B., Andrews, L., Curtis, J., and Dixon, W. E., "Saturated RISE Tracking Control of Store-Induced Limit Cycle Oscillations," *Proceedings of the AIAA Guidance, Navigation and Control Conference*, AIAA Paper 2013-4529, Aug. 2013.

[15] Patre, P. M., Mackunis, W., Makkar, C., and Dixon, W. E., "Asymptotic Tracking for Systems with Structured and Unstructured Uncertainties," *IEEE Transactions on Control Systems Technology*, Vol. 16, No. 2, 2008, pp. 373–379. doi:10.1109/TCST.2007.908227

[16] Fischer, N., Kan, Z., Kamalapurkar, R., and Dixon, W. E., "Saturated RISE Feedback Control for a Class of Second-Order Nonlinear Systems," *IEEE Transactions on Automatic Control* (to be published).

[17] Thompson, D. E. Jr., and Strganac, T. W., "Nonlinear Analysis of Store-Induced Limit Cycle Oscillations," *Nonlinear Dynamics*, Vol. 39, Nos. 1–2, 2005, pp. 159–178. doi:10.1007/s11071-005-1924-y

[18] Dixon, W. E., de Queiroz, M. S., Dawson, D. M., and Zhang, F., "Tracking Control of Robot Manipulators with Bounded Torque Inputs," *Robotica*, Vol. 17, No. 2, 1999, pp. 121–129. doi:10.1017/S0263574799001228

[19] Filippov, A., "Differential Equations with Discontinuous Right-Hand Sides," *American Mathematical Society Translations*, Vol. 42, No. 2, 1964, pp. 199–231.

[20] Smirnov, G. V., *Introduction to the Theory of Differential Inclusions*, American Mathematical Society, Providence, RI, 2002, pp. 87–116.

[21] Shevitz, D., and Paden, B., "Lyapunov Stability Theory of Nonsmooth Systems," *IEEE Transactions on Automatic Control*, Vol. 39, No. 9, 1994, pp. 1910–1914. doi:10.1109/9.317122

[22] Paden, B., and Sastry, S., "Calculus for Computing Filippov's Differential Inclusion with Application to the Variable Structure Control of Robot Manipulators," *IEEE Transactions on Circuits and Systems*, Vol. 34, No. 1, 1987, pp. 73–82. doi:10.1109/TCS.1987.1086038